Cell, Vol. 86, 35–46, July 12, 1996, Copyright ©1996 by Cell Press

Nuk Controls Pathfinding of Commissural Axons in the Mammalian Central Nervous System

Mark Henkemeyer,*§‖ Donata Orioli,‡‖ Jeffrey T. Henderson,* Tracy M. Saxton,*† John Roder,*† Tony Pawson,*† and Rüdiger Klein‡

*Programme in Molecular Biology and Cancer
Samuel Lunenfeld Research Institute
Mount Sinai Hospital
Toronto, Ontario
M5G 1X5 Canada

†Department of Molecular and Medical Genetics
University of Toronto
Toronto, Ontario
M5S 1A8 Canada

‡European Molecular Biology Laboratory
Meyerhofstrasse 1
D-69117 Heidelberg
Germany

Summary

Eph family receptor tyrosine kinases have been proposed to control axon guidance and fasciculation. To address the biological functions of the Eph family member Nuk, two mutations in the mouse germline have been generated: a protein null allele (*Nuk*^{1}) and an allele that encodes a Nuk-βgal fusion receptor lacking the tyrosine kinase and C-terminal domains (*Nuk*^{lacZ}). In *Nuk*^{1} homozygous brains, the majority of axons forming the posterior tract of the anterior commissure migrate aberrantly to the floor of the brain, resulting in a failure of cortical neurons to link the two temporal lobes. These results indicate that Nuk, a receptor that binds transmembrane ligands, plays a critical and unique role in the pathfinding of specific axons in the mammalian central nervous system.

Introduction

Receptor tyrosine kinases are involved in controlling cell growth and developmental fate decisions, in directing cell movement and migration, and in tissue morphogenesis (Pawson and Bernstein, 1990; Dickson and Hafen, 1994). The Eph family of receptor tyrosine kinases, which possesses at least 13 members, has been circumstantially implicated in regulating cell movement and axonal pathfinding (reviewed by Tuzi and Gullick, 1994; Brambilla and Klein, 1995; Tessier-Lavigne, 1995). Recently, considerable progress has been made in the identification of ligands for Eph receptors (or Lerks; Bartley et al., 1994; Beckmann et al., 1994; Cheng and Flanagan, 1994; Davis et al., 1994; Shao et al., 1994, 1995; Bennett et al., 1995; Bergemann et al., 1995; Drescher et al., 1995; Kozlosky et al., 1995; Winslow et al., 1995; Gale et al., submitted). All Lerks are anchored to the cell surface, either through a transmembrane segment in the case of Lerk2 (Elk-L/Efl-3/Cek5-L), Lerk5 (Htk-L/ELF-2), and Elk-L3, or through a glycosyl phosphatidylinositol (GPI) linkage for the other five known Lerks. Eph receptors can be subdivided into two classes based on their interactions with the various Lerks. The Elk, Nuk/Cek5, Sek4/Hek2, and Htk receptors (Elk subclass) all preferentially bind to and are activated by the transmembrane Lerks. Conversely, the remaining Eph receptors interact promiscuously with the GPI–linked Lerks and show little affinity for the transmembrane ligands (Brambilla et al., 1995; Gale et al., submitted). Interestingly, strong catalytic activation of Eph receptors can only be achieved by coculturing ligand-expressing cells with receptor-expressing cells, or by artificially oligomerizing soluble forms of the ligands (Davis et al., 1994). These results, as well as the immunolocalization of the Nuk receptor to specific sites of cell–cell contact, are consistent with the idea that this receptor–ligand family mediates close-range cellular interactions (Henkemeyer et al., 1994).

The properties of GPI–linked Lerks and their cognate receptors have provided clues to possible biological activities. B61 induces endothelial cell migration and can act as an angiogenic factor when applied to the rat cornea (Pandey et al., 1995). Two other GPI–linked Lerks, RAGS and ELF-1, are expressed in a posterior–to–anterior gradient in the chick tectum, and one of their receptors, Mek4, is expressed in a temporal–to–nasal countergradient in the retina (Drescher et al., 1995; Cheng et al., 1995). Moreover, membranes from the posterior tectum cause growth cone collapse of axons from the temporal retina, while recombinant RAGS repels the growth of retinal axons in vitro (Drescher et al., 1995). These observations have raised the possibility that Eph receptors and their ligands function as guidance molecules to establish a retinal–tectal topographic map. In separate studies, the human homolog of RAGS, AL-1, has been implicated in promoting the fasciculation of cultured cortical axons in vitro (Winslow et al., 1995).

We have previously identified and characterized Eph receptors of the Elk subclass, which bind to transmembrane ligands and are expressed to high levels in the nervous system (Letwin et al., 1988; Lhotak et al., 1991; Lhotak and Pawson, 1993, Henkemeyer et al., 1994; Gale et al., submitted). To investigate the biological functions of these receptors, we have introduced two mutations into the mouse *Nuk* gene and examined their effects on development of the nervous system. We find that Nuk plays a unique role during the pathfinding of a specific set of central nervous system axons forming the anterior commissure, a major interhemispheric connection between the two temporal lobes of the cerebral cortex.

Results

Nuk Mutations

The *Nuk*^{1} mutation was generated through homologous recombination in embryonic stem (ES) cells by deleting a 5′ segment of the *Nuk* locus and inserting a *neomycin* resistance cassette (Figure 1A). This deletion, which encompasses the exon for Nuk amino acids 29–50, was

§Present address: Center for Developmental Biology, University of Texas Southwestern Medical Center, Dallas, Texas 75235-9133

‖The first two authors made equal contributions to this work.

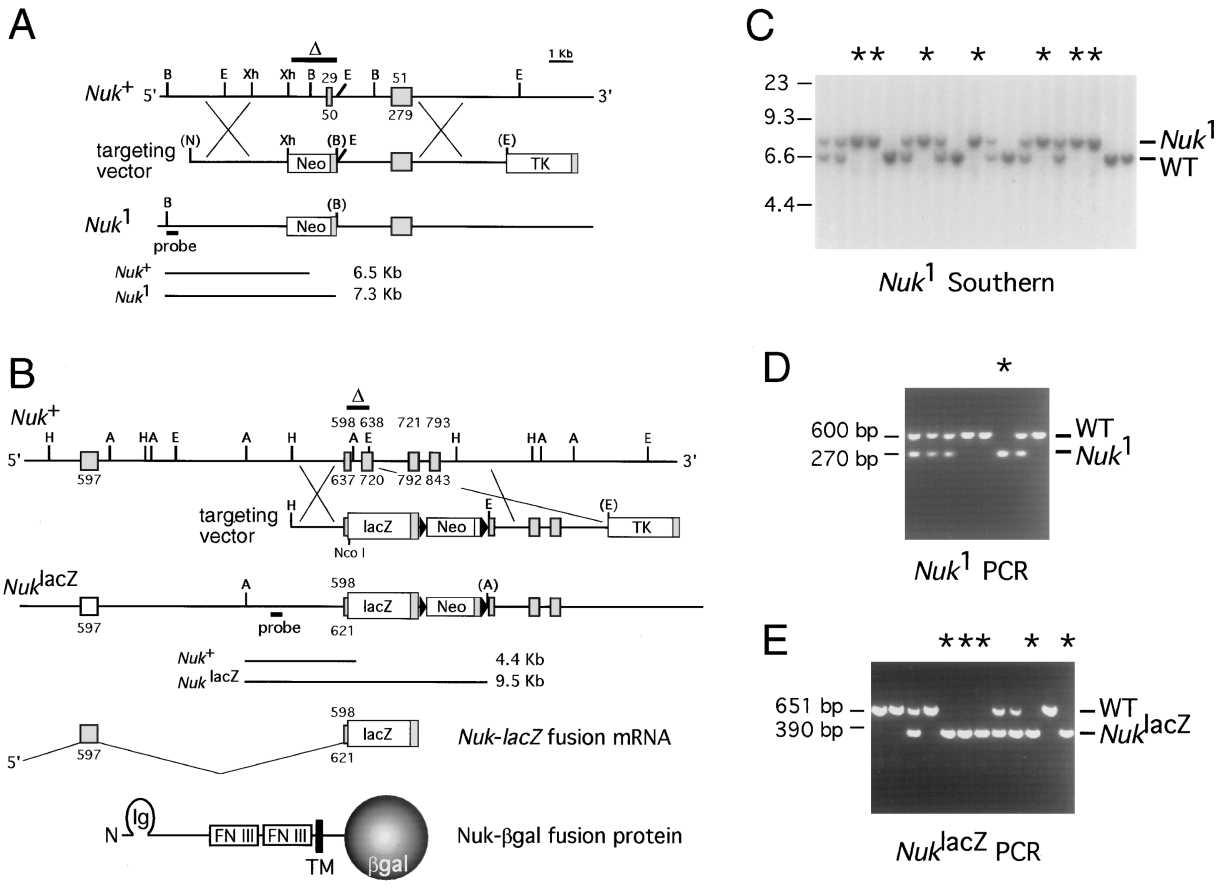

Figure 1. Generation of *Nuk*^{1} and *Nuk*^{lacZ} Mutations

(A) *Nuk*^{1} mutation. Genomic restriction map and targeting strategy used to delete a 1.4 kb region of *Nuk* containing the coding exon for Nuk amino acids 29–50. The *Nuk*^{1} targeting vector, including the PGK-*neo* and PGK-*tk* cassettes (boxes) and their transcription termination sequences (stippled boxes) are shown. Homologous recombinants were identified by hybridizing a 5′ external probe to BamHI digests of genomic DNA, resulting in a wild-type band of 6.5 kb and a *Nuk*^{1} mutant band of 7.3 kb. Pertinent restriction sites are indicated; those in brackets are derived from vector sequences. A, Asp-718; B, BamHI; E, EcoRI; H, HindIII; Xh, XhoI.

(B) *Nuk*^{lacZ} mutation. Genomic restriction map of a 3′ region of the *Nuk* locus containing exons encoding the Nuk juxtamembrane and tyrosine kinase domains. A group of four exons encoding Nuk amino acids 598–843 were identified (shaded boxes). A *Nuk-lacZ* targeting strategy was designed to delete 1 kb of *Nuk*, including codons for the ATP binding region of the tyrosine kinase domain (residues 622–707), while inserting in-frame bacterial *lacZ* including codons for the ATP binding region of the tyrosine kinase domain (residues 622–707). Homologous recombinants were identified by hybridizing a 5′ external probe with Asp-718 digests of genomic DNA, resulting in a wild-type band of 4.4 kb and a *Nuk*^{lacZ} mutant band of 9.5 kb. The predicted *Nuk-lacZ* mRNA and Nuk-βgal fusion protein are shown (TM, transmembrane).

(C–E) Genotype analysis of *Nuk*^{1} and *Nuk*^{lacZ} mutations.

(C) Southern blot analysis of *Nuk*^{1} mutant mice. Tail DNA from the offspring of intercrosses between *Nuk*^{1}/+ heterozygous males and females were digested with BamHI and subjected to Southern blot analysis, using the external probe shown in (A).

(D and E) Polymerase chain reaction analysis of *Nuk*^{1} (D) and *Nuk*^{lacZ} (E) mutant mice. The positions of wild-type (WT) and mutant bands are indicated, and asterisks denote the lanes where homozygote samples were loaded.

expected to generate a protein null allele, as sequence analysis indicated that any aberrant splicing around the *neo*^{r} cassette would result in a mutant transcript containing a frameshift in the *Nuk* open reading frame. The *Nuk*^{lacZ} mutant allele was designed to encode a fusion protein, comprised of the extracellular, transmembrane, and juxtamembrane domains of Nuk (amino acids 1–621) linked to β-galactosidase (βgal; Figure 1B). This Nuk-βgal fusion receptor lacks the entire tyrosine kinase catalytic and C-terminal domains of Nuk. Aggregation chimeras of three *Nuk*^{1}/+ and two *Nuk*^{lacZ}/+ targeted ES cell lines were generated, and germline transmission of the mutant alleles was obtained. Animals homozygous for either *Nuk* mutation were observed at the expected frequency in the progeny of heterozygous intercrosses and were identified by either Southern blot analysis or *Nuk*-specific polymerase chain reactions (Figures 1C–1E). *Nuk*^{1}/*Nuk*^{1} and *Nuk*^{lacZ}/*Nuk*^{lacZ} homozygotes were long-lived and fertile in 129 inbred and 129 × C57BL/6 or 129 × CD1 mixed backgrounds.

Biochemical Characterization of *Nuk*^{1} and *Nuk*^{lacZ} Alleles

To determine whether the *Nuk*^{1} mutation abrogated expression of the wild-type Nuk^{+} protein, antiserum raised

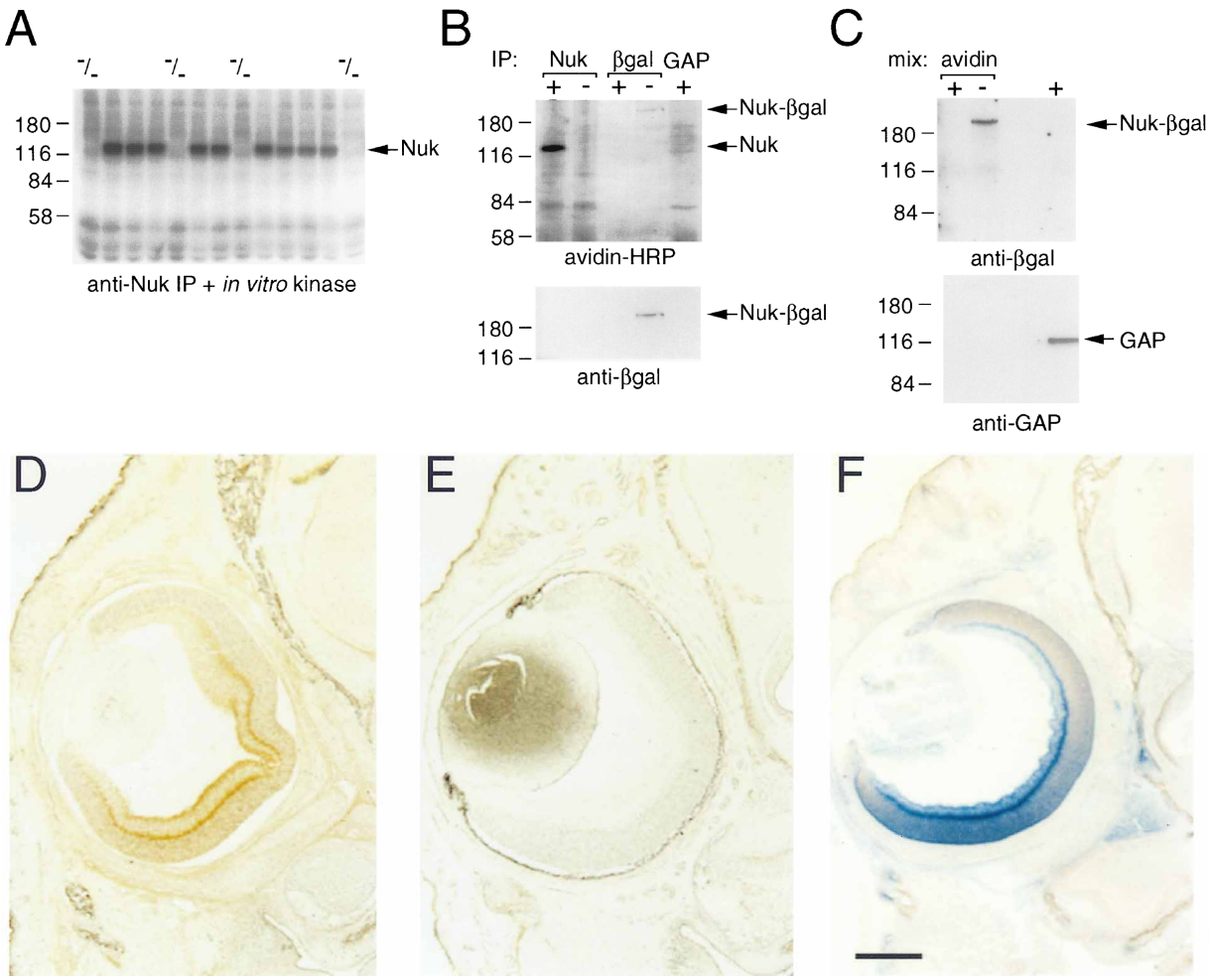

Figure 2. Biochemical Characterization of *Nuk*^{1} and *Nuk*^{lacZ} Mutations

(A) Nuk-specific in vitro kinase assays from E10.5 mouse embryos. Total protein lysates were prepared from individual embryos resulting from an intercross of *Nuk*^{1}/+ heterozygous males and females. Nuk protein was immunoprecipitated using anti-Nuk antibodies and subjected to in vitro kinase assays with γ-^{32}P ATP. Lanes containing homozygous (−/−) embryos are indicated.

(B and C) Biotinylation of cell-surface proteins from wild-type and *Nuk*^{lacZ} homozygous mutant brains. Cell-surface proteins from primary cultures of postnatal day 4 (P_4) brains were specifically biotinylated. In (B), total protein lysates from wild-type (+) and *Nuk*^{lacZ} homozygous (−) cultures were immunoprecipitated with anti-Nuk, anti-βgal, or anti-GAP antibodies and subjected to Western blot analysis with avidin conjugated to horseradish peroxidase or anti-βgal antibodies. In (C), total protein lysates from the cell surface biotinylated (+) and (−) cultures were incubated with avidin–agarose beads. The precipitated biotinylated proteins were then subjected to Western blot analysis using anti-βgal antibodies. The filter was subsequently stripped and reprobed with anti-GAP antibodies. The far right lane contains total cell protein lysate.

(D–F) Nuk^{+} and Nuk-βgal expression in coronal sections of the eye. Dorsal is up.

(D and E) Anti-Nuk antibody staining of +/+ (D) and *Nuk*^{lacZ}/*Nuk*^{lacZ} (E) newborn mouse heads.

(F) Nuk-βgal staining of a *Nuk*^{lacZ}/*Nuk*^{lacZ} newborn. Scale bar D–F, 400 μm.

against the Nuk C-terminus was used in an immune-complex in vitro tyrosine kinase assay. An autophosphorylated 130 kDa Nuk^{+} protein was specifically detected in +/+ and *Nuk*^{1}/+, but not in *Nuk*^{1}/*Nuk*^{1} embryo protein lysates (Figure 2A). No abnormally sized gene product was observed in *Nuk*^{1}/*Nuk*^{1} embryos that might result from readthrough past the *neo*^{r} cassette or from aberrant transcripts initiating downstream of the cassette. These results indicate the *Nuk*^{1} mutation is a protein null.

To investigate whether the *Nuk*^{lacZ} mutation led to the production of the expected 200 kDa membrane-bound Nuk-βgal fusion receptor, primary brain cultures from neonatal wild-type and homozygous mutants were obtained, and cell-surface proteins were specifically biotinylated. Total protein lysates were immunoprecipated with polyclonal antibodies directed against Nuk or βgal, and biotinylated species were detected in Western blots with avidin conjugated to horseradish peroxidase (HRP; Figure 2B). A 130 kDa protein that bound avidin was specifically precipitated from +/+ cells with anti-Nuk antibodies, indicating that Nuk^{+} was biotinylated and therefore exposed on the cell surface. In contrast, no biotinylated protein was precipitated with the anti-Nuk

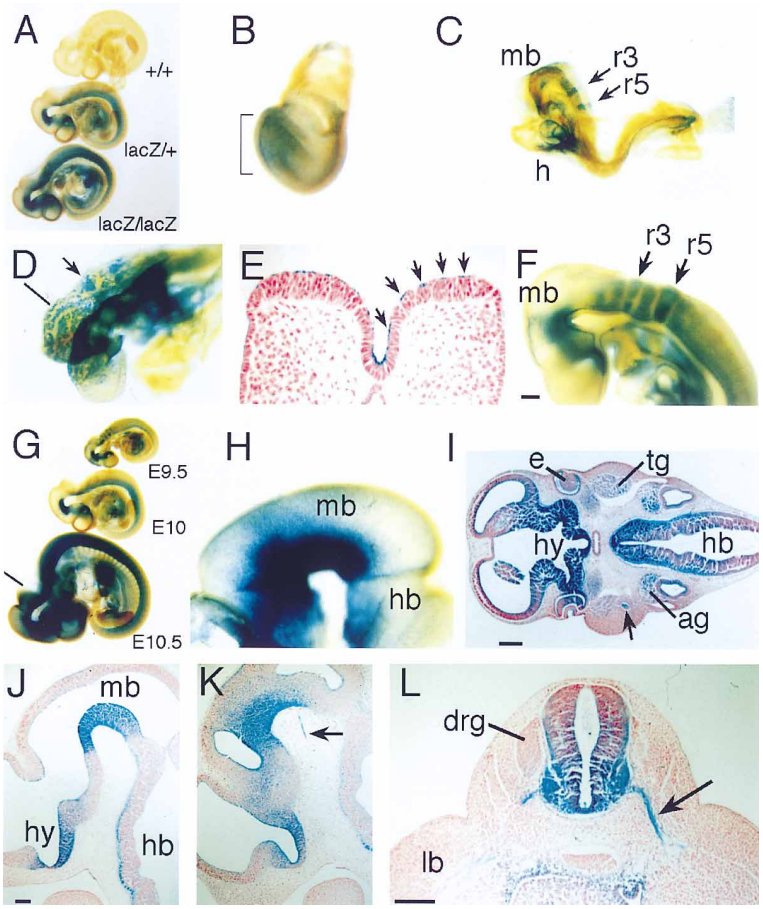

Figure 3. Expression of Nuk-βgal in the Developing Nervous System

Embryos containing the *Nuk*^{lacZ} mutation were collected and stained for Nuk-βgal activity and viewed as whole-mount specimens (A–D, F–H) or as tissue sections (E, I–L). Dorsal is up and anterior is left.

(A) +/+, *Nuk*^{lacZ}/+ and *Nuk*^{lacZ}/*Nuk*^{lacZ} E10 littermates. Nuk-βgal staining in *Nuk*^{lacZ}/+ and *Nuk*^{lacZ}/*Nuk*^{lacZ} embryos is mainly confined to the developing nervous system.

(B) At E7.5, Nuk-βgal was detected in the headfold process of the early nervous system (bracket).

(C) E8.5 embryos with 4 somites show Nuk-βgal staining in the neuroectoderm and heart (h). In the neural groove, staining was localized to the future forebrain, midbrain (mb) and hindbrain rhombomeres r3 and r5.

(D) Dorsal view looking down into the neural groove; the arrow points to r3, and the line indicates the plane of the transverse section shown in (E). (D) and (E) detail the repeating pattern of dorsal–ventral stripes of Nuk-βgal expression, localized to the apical/future ventricular surface of the neuroectodermal cells (arrows in E).

(F) At E9.25, Nuk-βgal intensely labeled specific ventral cells within the closed neural tube, including the hypothalamic region of the diencephalon, the tegmental region of the midbrain, and hindbrain rhombomeres.

(G) Between E9.5 to E10.5 days of development, embryos continue to express Nuk-βgal in the nervous system. (H–L) Nuk-βgal expression at E10.5.

(I and L) Transverse sections with the plane for (I) indicated by the line in (G) and the plane for (L) through the spinal region at the forelimb buds (lb).

(J and K) Two sagittal sections of the same embryo with (J) slightly off the midline and (K) approximately 200 μm lateral to (J). Nuk-βgal staining was intense in the preoptic area and hypothalamus (hy; I, J, K), the ventral midbrain (H, J, K), the ventral hindbrain (hb; H, I, and J), and the posterior neural tube (L). Note the near total absence of staining in dorsal cells. In (I), Nuk-βgal was also detected in the eye (e), the trigeminal (tg) and acoustic/vestibular (ag) ganglia, and the otic vesicle. Nuk-βgal localized within the axons of the PNS as shown for the trigeminal nerve entering branchial arch 1 (arrow in I), the oculomotor nerve whose cell bodies lie in the ventral midbrain (arrow in K), and the spinal motor nerves whose cell bodies lie in the ventral neural tube (arrow in L). The dorsal root ganglion (drg) did not express Nuk-βgal at E10.5. Scale bar F, J–L, 100 μm; I, 200 μm.

antibodies from *Nuk*^{lacZ}/*Nuk*^{lacZ} cells, as anticipated from the fact that the Nuk-βgal fusion protein lacks the C-terminal domain recognized by the anti-Nuk antibodies. However, the *Nuk*^{lacZ}/*Nuk*^{lacZ} cells did express a novel 200 kDa biotinylated polypeptide that was precipitated by anti-βgal antibodies. In the converse experiment, immobilized avidin precipitated a 200 kDa biotinylated protein specifically from *Nuk*^{lacZ}/*Nuk*^{lacZ} cultures that was recognized by anti-βgal antibodies (Figure 2C). The intracellular protein GAP did not become biotinylated, indicating that the labeling was indeed specific for proteins expressed on the surface of the plasma membrane. Thus, the *Nuk*^{lacZ} mutation leads to the expression of a 200 kDa Nuk-βgal fusion protein at the cell surface.

To test the fidelity with which the *Nuk*^{lacZ} allele was expressed, coronal sections of newborn eyes were subjected to anti-Nuk immunohistochemical analysis or stained for Nuk-βgal activity using the chromogenic substrate X-gal. Anti-Nuk antibodies revealed a ventral–to–dorsal gradient of Nuk^{+} expression in wild-type eyes (Figure 2D). In the retina, intense staining for Nuk^{+} protein was observed in the axon and dendrite-rich plexiform layer and in the ganglion cell axons forming the optic nerve. In eyes of a *Nuk*^{lacZ} homozygote no anti-Nuk immunoreactivity was detected (Figure 2E); however, staining for Nuk-βgal activity revealed an expression gradient and subcellular localization identical to Nuk^{+} (Figure 2F). This result and analysis of other specimens (see below) demonstrate that the Nuk-βgal fusion receptor is expressed in the same cell types and subcellular localizations previously described for the endogenous Nuk^{+} protein (Henkemeyer et al., 1994).

Nuk-βgal Expression in the Early Nervous System

The Nuk-βgal fusion receptor provides a very precise and sensitive means to characterize Nuk expression. As shown for mid-gestation E10 specimens, Nuk-βgal staining was detected in *Nuk*^{lacZ}/+ and *Nuk*^{lacZ}/*Nuk*^{lacZ}, but not +/+, embryos (Figure 3A). At earlier stages, Nuk-βgal was confined to the headfolds (Figure 3B), which by

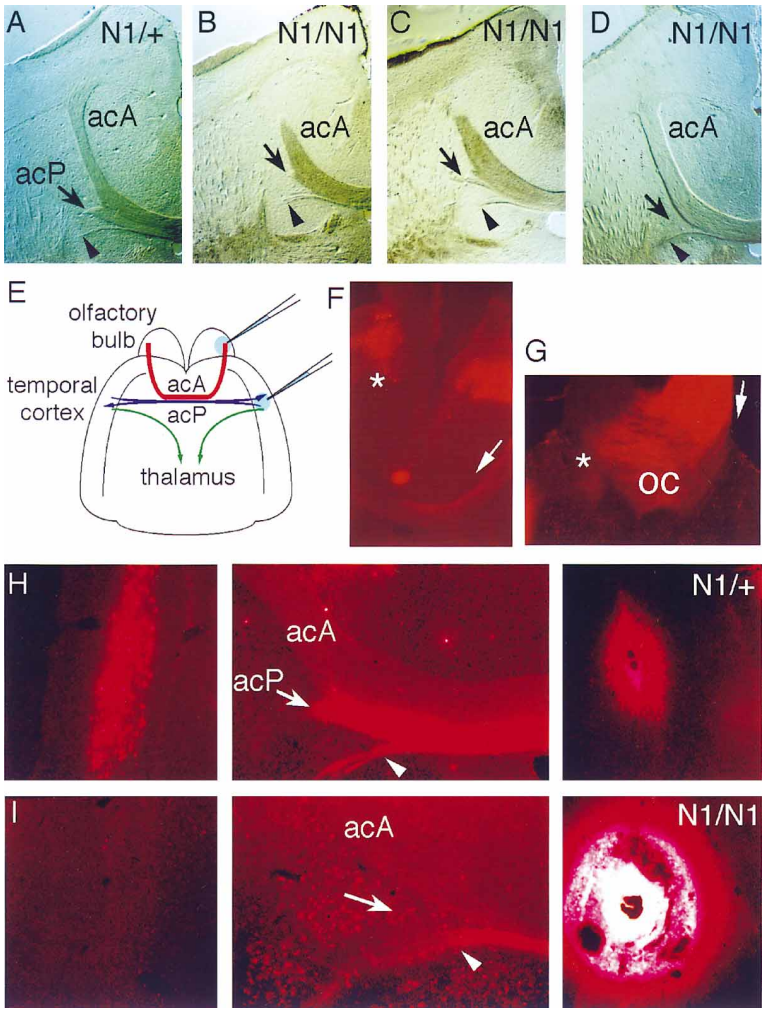

Figure 4. Defective Anterior Commissure in *Nuk*^{1} Homozygotes

(A–D) Horizontal sections through the anterior commissure in a *Nuk*^{1}/+ (A) and three different *Nuk*^{1}/*Nuk*^{1} (B–D) adult brains. Anterior is up, and only the left hemisphere of each forebrain is shown. Axon bundles were visualized using interference microscopy. In (A), large acA and acP (arrow) tracts can be observed. In (B)–(D), axon fibers forming the acP tract were absent or much reduced (arrows). A third much smaller tract that is not affected by the *Nuk*^{1} mutation can also be identified behind the acP fibers (arrowheads).

(E–I) *In vivo* dye tracing of the anterior commissure and optic nerve in adult mice.

(E) Diagram outlining the brain and the strategy used to trace the acP and acA axons with fluorescent dyes. The left olfactory bulb and temporal cortex are indicated, as are their associated commissural axon tracts.

(F) Dye injection into an olfactory bulb of a *Nuk*^{1}/*Nuk*^{1} animal properly traced the axons in the acA tract (arrow) and labeled cells in the contralateral olfactory bulb (asterisk).

(G) Dye injection into the retina of a *Nuk*^{1}/*Nuk*^{1} animal traced the axons in the optic nerve (arrow) as they near the optic chiasma (oc). As in wild-type mice, a majority of the labeled retinal ganglion cell axons in *Nuk*^{1} mutants crossed the midline in the chiasma (asterisk).

(H and I) Injections of dye into the temporal cortex were used to label the acP axons. The right panels show the site of injection, the middle panels show sections at the midline where the acA and acP tracts converge, and the left panels show sections of the contralateral temporal cortex.

(H) In a *Nuk*^{1}/+ specimen, the acP tract was labeled (arrow), as were cells in the contralateral cortex (left panel), indicating a functional anterior commissure.

(I) In a *Nuk*^{1}/*Nuk*^{1} mutant, dye did not label the reduced acP tract (arrow) or cells in the contralateral cortex (left panel). Note that the small posterior tract unaffected by the *Nuk*^{1} mutation also was labeled by the injections into the temporal cortex (arrowhead in middle panels). The acA tract was not labeled by injections into the temporal cortex.

E8.5 resolved into a highly ordered expression pattern in the neuroectodermal cells of the neural plate (Figures 3C–3E). Intense staining was detected in specific anterior–posterior regions of the future brain, including the ventral midbrain and hindbrain rhombomeres r3 and r5. Interestingly, this staining also revealed at high resolution a pattern of longitudinal stripes of Nuk-βgal–expressing and nonexpressing cells down the length of the future brain (see Figures 3D and 3E). Thus, Nuk expression in the open neural groove marks specific anterior–posterior and dorsal–ventral cells.

Following dorsal closure, Nuk-βgal expression intensified in defined regions of the forebrain, midbrain, and rhombomeres r3 and r5, with relatively lower expression detected in the other hindbrain segments and in the posterior neural tube (Figures 3F–3L). The most intense Nuk-βgal staining was restricted to ventral structures, most notably in the preoptic area and hypothalamus of the forebrain (Figures 3I and 3J), the tegmental region of the midbrain (Figures 3H and 3J), the ventral hindbrain (Figure 3I), and the ventral neural tube throughout the length of the spinal cord (Figure 3L). Like the Nuk^{+} receptor (Henkemeyer et al., 1994), the Nuk-βgal fusion protein localized to early axon fibers of the peripheral nervous system (PNS), including the trigeminal nerves (Figure 3I), the oculomotor nerves (Figure 3K), and the spinal motor nerves (Figure 3L). Nuk is therefore most highly expressed in ventral cells of the neural tube and within axons of the PNS.

Axon Pathfinding Defect in *Nuk*^{1} Mutant Brains

Histological analysis of serial sections through a number of *Nuk*^{1}/*Nuk*^{1} brains revealed defects in a specific axon tract of the forebrain. In all 16 specimens examined, there was a striking reduction in the lateral projection of the anterior commissure. A section through the forebrain of a *Nuk*^{1}/+ adult mouse (Figure 4A) exhibited a normal anterior commissure, composed of two major axon pathways: a horseshoe-shaped tract connecting the two olfactory bulbs (pars anterior, acA) and a lateral tract with projections between the two temporal lobes (pars posterior, acP). Sections at similar levels through

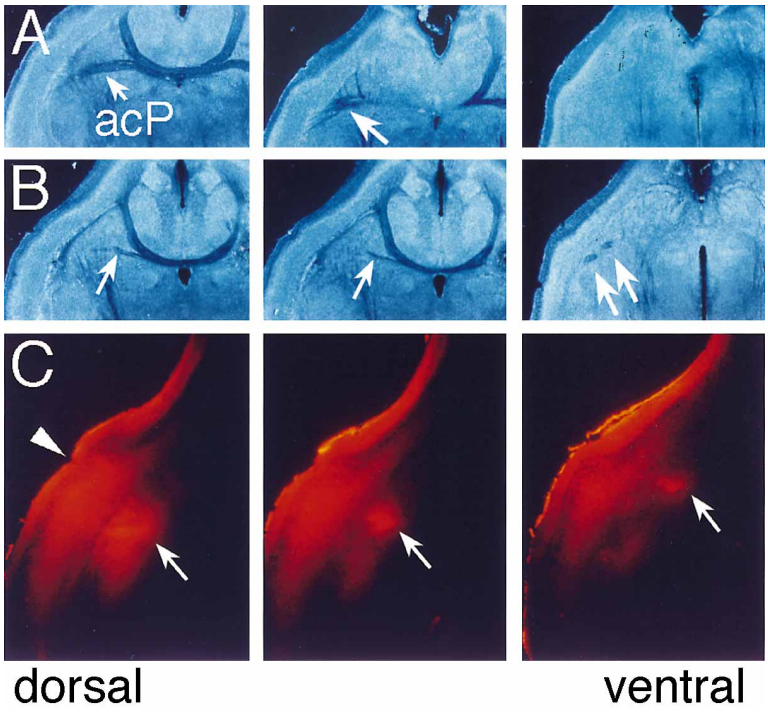

Figure 5. Abnormal Migration of acP Axons in *Nuk*^{1} Homozygotes

(A and B) Serial horizontal sections of neonatal (P_5) brains at the level of the anterior commissure viewed under interference contrast microscopy. Sections (3) of each specimen are shown with the most ventral section depicting the floor of the brain on the right and more dorsal sections to the left.

(A) In a *Nuk*^{1}/+ brain, the acA and acP tracts have formed thick bands of fibers crossing the midline. The acP tract is marked by arrows.

(B) A much reduced acP tract was evident in the brain of a *Nuk*^{1}/*Nuk*^{1} littermate (arrows). In the most ventral section, groups of bundled axons were observed to have abnormally migrated towards the floor of the brain (paired arrows).

(C) Dye tracing of the temporal cortex in a *Nuk*^{1}/*Nuk*^{1} neonatal (P_5) brain. DiI crystals were placed into the temporal cortex of fixed brains and allowed to trace the cortical axon fibers. Fluorescent images of horizontal sections corresponding to the ventral-most floor of the brain of one mutant are shown. The site of DiI placement in the temporal cortex is indicated (arrowhead). These sections document accumulations of DiI-labeled cortical axons that have migrated improperly towards the floor of the brain (arrows).

Nuk^1/*Nuk*^{1} adult brains revealed a marked reduction of the acP axon tract (Figures 4B–4D). In adult brains, the acP tract was over 300 μm thick, whereas, in all cases examined, the acP in *Nuk*^{1}/*Nuk*^{1} homozygotes was reduced to less than 100 μm. The specificity of this defect to the acP tract was highlighted by the presence of a normal acA tract in the mutants.

To analyze this phenotype in greater detail, in vivo axon tracing experiments were performed on major forebrain commissures, using vital fluorescent dyes. In separate experiments, axons corresponding to the acP tract, acA tract, corpus callosum, or optic nerve were labeled by injecting a small amount of dye into the appropriate location of deeply anesthetized mice (Figure 4E). Injected dye was then allowed to trace the axons in revived animals for 48 hr, after which brain tissues were serially sectioned and viewed under fluorescent microscopy. For the acA tract (Figure 4F), the corpus callosum (data not shown), and the optic nerve (Figure 4G), dye-tracing experiments revealed that labeled axons had properly crossed the midline to form normal functional pathways. To analyze the axonal projections of the acP tract, Fast Blue was injected into the pyramidal layer of the temporal cortex. As shown for a *Nuk*^{1}/+ brain, a small amount of injected Fast Blue readily traced the acP tract and labeled neurons in the contralateral temporal cortex (Figure 4H). However, as the acP tract is much reduced in *Nuk*^{1}/*Nuk*^{1} homozygotes, few if any Fast Blue–labeled neurons were observed in the contralateral temporal lobe of mutant brains even when greater amounts of the dye were injected (n = 6; Figure 4I).

To understand whether the acP tract forms normally and then degenerates later in life or whether it fails to form during embryonic development, we analyzed neonatal brains by serial sectioning and dye-tracing studies. In brains from +/+ and *Nuk*^{1}/+ animals, the acA and acP tracts were well formed, projecting through the midline into their contralateral targets (Figure 5A). However, in brains from *Nuk*^{1}/*Nuk*^{1} littermates, only the acA tract was well developed (Figure 5B). In all mutants examined, a much reduced number of acP axon fibers was observed to have migrated towards the midline. Instead, the majority of these axons appeared to have migrated as fasciculated bundles into the ventral floor of the forebrain (Figure 5B, right). To confirm that these axons were inappropriate projections of cortical neurons, Fast DiI was stereotatically placed into the temporal cortex of neonatal brains and allowed to trace in vitro for 6 weeks. For all four *Nuk*^{1}/*Nuk*^{1} brains analyzed, misdirected axonal material was observed to label the ventral forebrain adjacent to the site of dye placement (Figure 5C). This confirms that the defect in the acP tract associated with the *Nuk*^{1} mutation is primarily due to a failure of the temporal cortical neurons to extend axons laterally towards the midline and subsequently into the contralateral cortex.

Nuk^{lacZ} Homozygotes Can Exhibit a Normal Anterior Commissure

The brains of adult and newborn mice homozygous for the *Nuk*^{lacZ} mutation were also analyzed for the presence of an intact anterior commissure. Since the Nuk-βgal fusion protein lacks the Nuk tyrosine kinase catalytic domain, it might be anticipated that *Nuk*^{lacZ} homozygotes would show the same defect as the *Nuk*^{1} mutants. However, in 129 inbred or 129 × CD1 mixed backgrounds, all *Nuk*^{lacZ}/*Nuk*^{lacZ} adult brains examined (n = 12) had

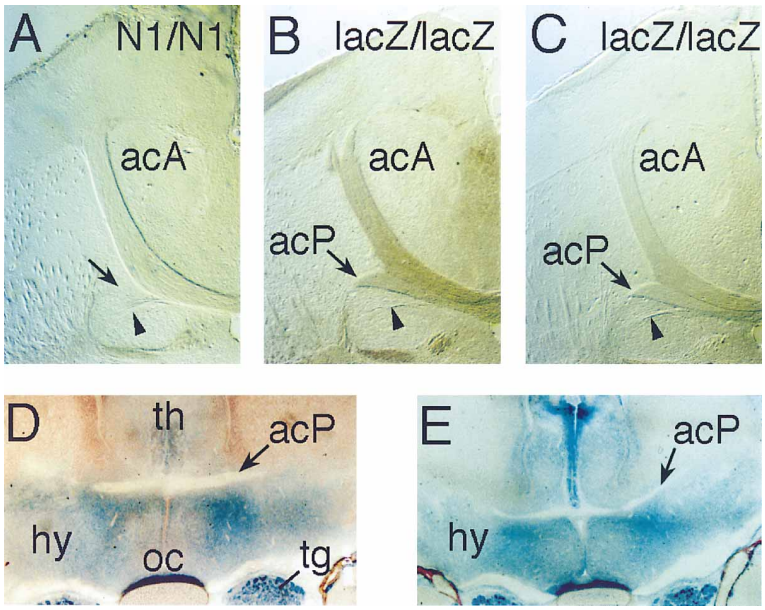

Figure 6. *Nuk*^{lacZ} Homozygotes Exhibit a Normal acP Pathway

(A–C) Horizontal sections through the anterior commissure of a *Nuk*^{1}/*Nuk*^{1} (A) and two different 129 × CD1 *Nuk*^{lacZ}/*Nuk*^{lacZ} (B and C) adult brains. Interference microscopy revealed a normal bundle of acP axons crossing the midline in the *Nuk*^{lacZ} homozygotes (arrows).

(D and E) Coronal sections of *Nuk*^{lacZ}/*Nuk*^{lacZ} newborn (D) and E16.5 day (E) specimens. The acP tracts were well formed, appearing as a white bundle crossing the midline. These sections were stained for Nuk-βgal, indicating that in this region of the brain, *Nuk* is most highly expressed in cells of the preoptic area and hypothalamus (hy), which lie directly underneath the acP tract. The acP axons did not stain for Nuk-βgal activity. In these sections, Nuk-βgal staining was localized to retinal ganglion axons in the optic chiasma (oc), in the trigeminal ganglia (tg), and, to a lesser extent, in the thalamus (th).

a normal acP fiber tract (Figure 6). Dye tracing of the temporal cortex further confirmed the presence of a normal acP axon pathway in these brains (data not shown). Volumetric reconstructions from morphometric analysis of the acP tract showed no difference between wild-type and *Nuk*^{lacZ}/*Nuk*^{lacZ} mice, while *Nuk*^{1}/*Nuk*^{1} mice exhibited up to an 80% reduction in the morphometric volume of the tract (data not shown). The acP tract in the *Nuk*^{lacZ}/*Nuk*^{lacz} mutants formed normally during embryonic development and could easily be detected in newborn and E16.5 day specimens (Figures 6D and 6E). These results indicate that a truncated Nuk receptor lacking the tyrosine kinase catalytic domain retains functions required for the pathfinding of temporal cortical axons.

Nuk Expression Marks the Path of acP Axons in the Forebrain

The expression of Nuk in the embryonic forebrain during the stages of acP axon migration and pathfinding was carefully analyzed using both anti-Nuk immunohistochemistry (data not shown) and by staining for Nuk-βgal activity (Figure 7). At E14.5, high expression of Nuk was detected specifically within the cells of the hypothalamus and preoptic area directly underneath the acP axon fibers. Remarkably, there was very little to no expression in the acP axon bundles or in the cells of the brain directly above the commissure (see also Figure 6D). The acP axons appear to have traversed above the Nuk-expressing cells in the hypothalamus and preoptic area such that by E14.5 the leading growth cones have reached the midline, which has yet to fuse and remains separated by the third ventricle. As these axons accumulate near the midline, transient structures form similar to Probst's bundles (Probst, 1901), which appear to be bounded both below and above by Nuk-expressing cells (see Figures 7D and 7G). By E15.5, acP axons from both sides will have crossed the midline to migrate along the tract set up by the corresponding contralateral partner tract. Thus, the acP axons appear to migrate preferentially along a pathway defined by Nuk expression in the basal forebrain, in such a fashion that these axons do not migrate into the Nuk expression domain. Moreover, in *Nuk*^{1} homozygotes, the acP axons inappropriately migrate into this region, which would normally express Nuk.

Transmembrane Ligands Are Detected in the Anterior Commissure

The apparent lack of Nuk expression in the axons forming the acP tract prompted us to examine the expression of the transmembrane ligands that bind Nuk. Antibodies raised against a peptide corresponding to a unique region of the Lerk2 extracellular domain were used to characterize its expression in the forebrain. To test the specificity of this antibody, protein lysates of Lerk2 and Lerk5–transfected Cos1 cells were immunoblotted, and a protein of the expected 38 kDa was detected only in Lerk2-transfected cells (S. Holland, G. Mbamalu, N. Gale, G. Yancopoulos, M. H., and T. P. unpublished data). Anti-Lerk2 immunohistochemistry specifically labeled the acA and acP tracts of the anterior commissure (Figure 8). In related experiments, the extracellular portions of the Elk and Nuk receptors were used as Fc-conjugated affinity reagents to probe for expression of Lerks. These reagents also labeled the anterior commissure, providing further evidence for Lerk expression in this particular axon tract (data not shown).

Discussion

Over the past century, a key interest of developmental neurobiology has been the formation of commissural axon tracts in the brain and spinal cord (Mihalkovics, 1877; His, 1889; Langelaan, 1908; Von Szily, 1912; Johnston, 1913; Suitsu, 1920; Silver et al., 1982; Katz et al., 1983). The results presented in this paper show that Nuk, a member of the Eph receptor tyrosine kinase family that

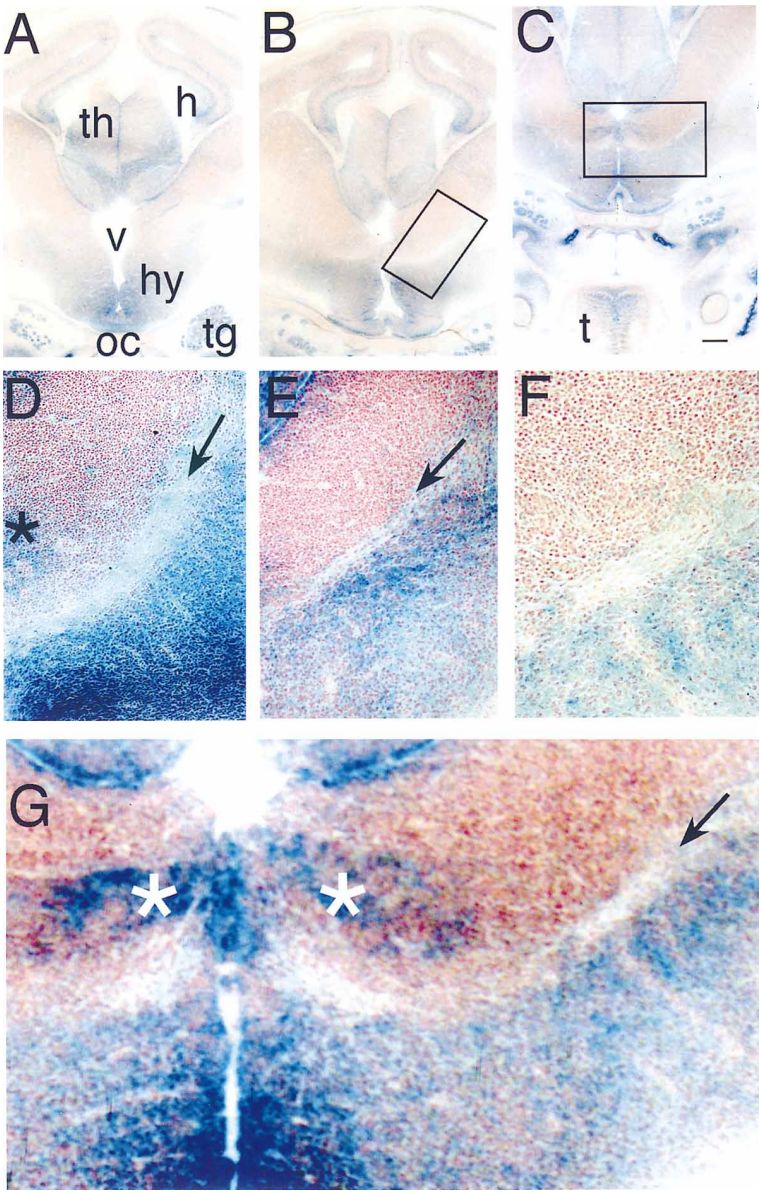

Figure 7. Expression of Nuk-βgal in the Forebrain at E14.5

Coronal sections through the forebrain of 129 × CD1 Nuk^{lacZ}/Nuk^{lacZ} embryos were stained for Nuk-βgal activity.

(A–C) Low magnification sections through the forebrain with (A) a more caudal/posterior section than (B) or (C). Nuk-βgal staining was detected in the hypothalamus (hy), the thalamus (th), the hippocampus (h), the optic chiasma (oc), the trigeminal ganglion (tg), and tongue (t). In the more posterior section (A), Nuk expression was detected throughout the hypothalamus, while in sections bisecting the acP tract (B and C), Nuk is restricted to ventral cells.

(D–G) High magnification views of the acP tract. The boxed area in (B) is shown in (D), and the boxed area in (C) is shown in (F) and (G). The axons forming the acP tract appear as white bundled fibers migrating from the temporal cortex through the forebrain, gradually curving toward the midline (arrows). Nuk-βgal was detected in the cells of the hypothalamus underneath the acP and was not observed to label the axons themselves. The only region where strong Nuk-βgal staining was detected above the acP axon fibers was in a patch of cells at the midline, directly above the growth cones that accumulate prior to midline fusion (asterisks in [D] and [G]). Scale bars: A–C, 200 μm; D, E, 50 μm; F, 25 μm.

binds transmembrane ligands, plays a unique role in the guidance of cortical axons that form the anterior commissure. The normal trajectory of these axons correlates with a boundary of Nuk expression in the ventral region of the brain, underlying the path of this commissure.

Nuk Is Required for Pathfinding of the Anterior Commissure

In mice homozygous for the Nuk^{1} protein-null mutation, the cortical axons forming the acP tract are misrouted and appear to project as fasciculated bundles into the ventral floor of the brain. Fluorescent dye-tracing studies of the cortical neurons that form the anterior commissure have confirmed a functional defect in communication between the two lobes of the temporal cortex. These observations provide direct evidence that Eph receptors are involved in the guidance and pathfinding of central nervous system axons. For Nuk, this function appears to be specific for the acP tract, as other axon pathways appeared normal in the mutant brains, including the partner acA component of the anterior commissure.

A surprising finding is that correct pathfinding of the acP axons in 129 or CD1 mice can be supported by a truncated Nuk receptor that lacks the kinase domain. These results are not without precedent. In Drosophila, the essential functions of the abl cytoplasmic tyrosine kinase are also independent of its catalytic activity (Henkemeyer et al., 1990). Indeed, tyrosine kinase–inactive forms of abl that exhibit proper subcellular localization to axons can rescue the lethality, sterility, and rough-eye phenotypes of *abl* mutant flies. The abl kinase activity does become essential when the *abl* mutations are combined with mutations in interacting loci, including the gene *disabled*. Similarly, essential functions for Nuk tyrosine kinase activity have been revealed by the finding that both the Nuk^{1} and Nuk^{lacZ} mutations exhibit similar double-mutant phenotypes when combined with a

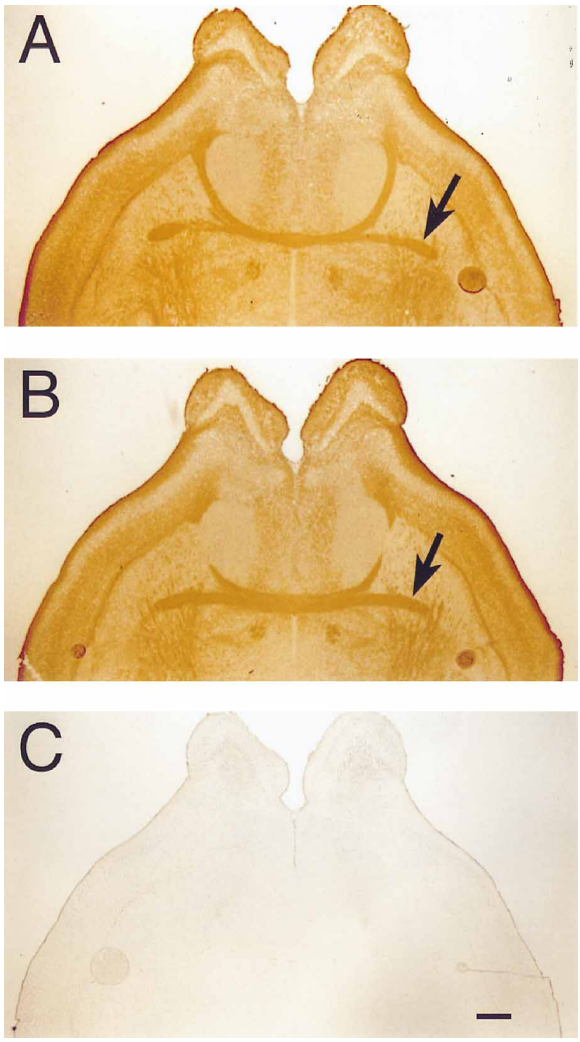

Figure 8. Expression of Lerk2 in the Forebrain

Horizontal sections of newborn brains were probed with affinity-purified anti-Lerk2 antibodies.

(A and B) The acP (arrows) and acA tracts of the anterior commissure were labeled.

(C) Preincubating the anti-Lerk2 antibody with the immunizing peptide abolished all staining. Scale bar: 400 μm.

mutation in the related *Sek4* gene (Orioli et al., submitted). Furthermore, in a C57BL/6 genetic background, the *Nuk*^{lacZ} mutation induced a defect in the anterior commissure (our unpublished data), suggesting that the Nuk kinase domain may play a role in acP pathfinding that is only evident in specific mouse strains.

How Does Nuk Guide acP Axons?

The defective pathfinding of the acP axons is consistent with the restricted expression of Nuk in the ventral forebrain. Even during early stages of neural development, the highest levels of Nuk protein are found in the ventralmost cells along the midline of the neural plate. Moreover, as the neural tube closes (and throughout embryonic development), the brain and spinal cord continue to express Nuk almost solely in ventral-cell types, with the most intense levels being detected in the forebrain and midbrain (see Figures 3H and 3J). Well before the birth of the cortical neurons that will extend acP axons, the early expression of Nuk in the ventral forebrain marks cells that will eventually form the preoptic area and hypothalamus.

An expectation arising from the defect in acP axon guidance in *Nuk*^{1} homozygous mice is that Nuk should be expressed in the commissural axons and function in these cells to control growth cone motility in response to transmembrane ligands in surrounding cells. However, expression analysis of Nuk and its ligands in the region of the developing commissure indicates that this scheme may be too simplistic. Nuk was not detected at significant levels in the acP axon fibers themselves. Instead, we found high levels of Nuk expressed specifically in cells of the preoptic area and hypothalamus immediately ventral to the commissure. In contrast, transmembrane ligands (i.e., Lerk2) were identified in the acP axons. Hence, although it is possible that a low level of Nuk is present and functions in the acP axons, an alternative model is that correct pathfinding of axons forming the anterior commissure depends on Nuk expression in the ventral cells over which the acP axons migrate. This latter hypothesis is more consistent with the expression data of Nuk and its ligands. Thus, the role of Nuk in guiding acP axons may not be cell-autonomous, in the sense that Nuk is not significantly expressed in the axons that are affected by the *Nuk*^{1} mutation.

As shown in Figure 7, by E14.5 the axons of the anterior commissure have migrated from the temporal cortex across one side of the brain, and their growth cones accumulate near the midline. In these sections, Nuk expression in the preoptic area and hypothalamus appeared to mark a pathway along which the acP axons migrate. In wild-type and *Nuk*^{lacZ} homozygotes, very few axon fibers were observed to stray from this trajectory and project into the Nuk-expression domain. However, in *Nuk*^{1} homozygotes, the great majority of the acP axons migrated aberrantly, projecting down into the region of the ventral forebrain that would normally express Nuk. The most straightforward interpretation of these observations is that the Nuk receptor exerts a repulsive function that prevents acP axons from migrating ventrally into the preoptic area and hypothalamus.

Support for the idea that Nuk provides a cue to guide acP axons came from a close examination of Nuk expression along the path of the developing axon tract, which indicated that a small pocket of nonexpressing cells formed near the midline (Figure 7G). The growth cones of the acP axon fibers appear to migrate into this pocket and to accumulate prior to fusion of the midline, in an area where they are bounded by Nuk-expressing cells on all sides. Midline fusion would then provide a route for the axons to cross and migrate towards the contralateral cortex. In the scheme proposed above in which Nuk may have a repulsive effect on axon migration, Nuk expression can be envisaged as forming a conduit that, through its inhibitory effects, would force the migration of acP axons towards and ultimately across the midline.

The suggestion that Nuk acts in cells in the brain ventral to the acP tract, rather than in the axons themselves, may explain the finding that these axons project normally to their contralateral targets in 129 and CD1

Nuk^{lacZ} homozygotes. The ability of the Nuk-βgal fusion to promote normal pathfinding of the anterior commissure suggests that the extracellular, transmembrane, or juxtamembrane regions of Nuk are critical for acP guidance, and that the tyrosine kinase catalytic domain is not.

How might the kinase-defective Nuk-βgal fusion protein control axon guidance? It is possible that Nuk-βgal, which retains the juxtamembrane region containing potential autophosphorylation sites, can form heterodimers with other Eph receptors such as Sek4 and thereby contribute to intracellular signaling and axon pathfinding. However, as neither Nuk^{+} nor Nuk-βgal are significantly localized to the acP axons, they are unlikely to act in a cell-autonomous fashion within the anterior commissure. Conceivably, Nuk-βgal, by heterodimerizing with other Eph family receptors, could function in the preoptic area and hypothalamus to regulate cell adhesion molecules involved in axon migration. However, since βgal is only catalytically active as a tetramer, the Nuk-βgal fusion protein must homooligomerize through its βgal moiety, perhaps interfering with its ability to heterodimerize with other Eph receptors. This may explain why Nuk-βgal does not exhibit a dominant-negative phenotype, even though this might have been anticipated (Xu et al., 1995).

An alternative explanation for our observations is that the extracellular domain of Nuk^{+} or Nuk-βgal, when expressed on the surface of cells in the preoptic area and hypothalamus, provides a direct signal that guides the migration of acP axons. This could be achieved if transmembrane Lerks, which are apparently expressed on acP axons, themselves function as signaling molecules upon interaction with the Nuk extracellular domain. Both Lerk2 and Lerk5 have highly conserved 83 amino acid cytoplasmic domains and are identical in their C-terminal 33 residues, including several potential tyrosine phosphorylation sites (Beckmann et al., 1994; Davis et al., 1994; Fletcher et al., 1994; Shao et al., 1994; Bennett et al., 1995; Bergemann et al., 1995; Kozlosky et al., 1995). Furthermore, we have noted that both Lerk2 and Lerk5 become highly phosphorylated on tyrosine when coexpressed in Cos cells with an activated Src cytoplasmic tyrosine kinase (S. Holland, G. Mbamalu, N. Gale, G. Yancopoulos, M. H., and T. P., unpublished data). By receiving guidance cues from the Nuk extracellular domain, transmembrane Lerks might then transduce these signals into the acP axons, potentially in conjunction with a tyrosine kinase, resulting in a modification of their migration and pathfinding. This scheme is clearly not incompatible with a signal being transmitted by Nuk into the Nuk-expressing cells upon contact with the corresponding Lerks. Nuk has been shown to localize at sites of cell–cell contact (Henkemeyer et al., 1994), and Lerks are known to stimulate the tyrosine kinase activity of receptors only upon clustering or membrane attachment (Davis et al., 1994). Thus, it is possible that Nuk and its transmembrane ligands function in bidirectional signal transduction pathways activated at sites of cell–cell junctions.

Multiple Functions for Eph Receptors and Their Ligands

Nuk is highly localized in the axons of retinal ganglion cells and in the axonal compartment of a broad range of sensory and motor neurons in the PNS (Henkemeyer et al., 1994; data not shown). This suggests that Nuk may act directly within these axons to control neuronal pathfinding or targeting. The lack of any obvious phenotype affecting these structures in *Nuk*^{1} or *Nuk*^{lacZ} homozygous mutant mice may be due to the compensating effects of other Eph receptors. The Eph receptor Mek4, which binds GPI–linked ligands, is expressed in a temporal–to–nasal gradient in the chick retina, and the Lerks, RAGS, and ELF-1 have been detected in posterior–to–anterior gradients in the tectum (Cheng et al., 1995; Drescher et al., 1995). Furthermore, cells expressing RAGS induce retinal axons to undergo growth cone collapse in vitro (Drescher et al., 1995). These observations have led to suggestions that Eph receptors act in retinal axons to control pathfinding and that repulsive activities of the GPI–linked Lerks may function to establish a topographic map of the retina in the brain. Interestingly, we have also observed a gradient of Nuk expression in the retina; however, this receptor forms a ventral–to–dorsal gradient. This raises the possibility that the two different classes of Eph receptors and ligands may serve complementary functions during the pathfinding of retinal ganglion cell axons. Experiments are in progress to investigate whether the retinal–tectal map is affected in *Nuk*-mutant mice.

A direct analysis of Eph receptor function by targeted mutation of the *Nuk* gene in mice has revealed a profound defect in the pathfinding of a specific axon tract of the anterior commissure. While our results show that Eph receptors are indeed important for directing axon migration in the central nervous system, they also indicate that the functions of Eph receptors and their ligands in the brain may be more complex than proposed for the PNS or retinal–tectal system. This is suggested by the finding that Nuk is strongly expressed by cells of the brain immediately ventral to the acP migration route, while the transmembrane Lerks are highly localized to the axons of cortical neurons, and by the observation that a kinase-defective form of Nuk can suffice to support normal pathfinding of the acP fibers. These results suggest that Eph receptors and their ligands play a dynamic role in controlling cell movements in the developing nervous system.

Experimental Procedures

Nuk Gene Targeting

The *Nuk*^{1} targeting vector was constructed by inserting 4 kb and 6.6 kb fragments of cloned 129 strain genomic DNA from the 5′ end of the *Nuk* gene into pPNT (Tybulewicz et al., 1991). To construct the *Nuk-lacZ* targeting vector, we first modified a 2.5 kb genomic fragment of *Nuk* by site-specific mutagenesis to contain an NcoI restriction site in the exon sequence at codon 622. The NcoI site was then used to fuse this *Nuk* exon in-frame with a 3.5 kb *lacZ* cassette (pATG*lacZ*) that also contains at the 3′ end an SV40 eukaryotic polyadenylation sequence (Calzonetti et al., 1995). This 6 kb *Nuk-lacZ* fragment served as the 5′ arm and was cloned into pPNT. The 3′ arm consisting of a 5 kb *Nuk* genomic fragment was subsequently inserted between the *neo* and *tk* selection cassettes. Linearized targeting vectors were electroporated into the ES cell line RI (Nagy et al., 1993), and colonies were isolated following selection in G418 and gancyclovir (Wurst and Joyner, 1993), expanded, and genomic DNA screened by Southern blotting. The frequency of homologous recombination was 10 of 215 (*Nuk*^{1}) and 3 of 125 (*Nuk*^{lacZ}) cell lines screened. Germline transmission was obtained by generating aggregation chimeras with targeted ES cells (Nagy et al., 1993).

Biochemical Analysis

For the in vitro kinase assay, individual embryos were collected, and yolk sac DNA was used to genotype for the *Nuk*^{1} mutation. Embryo lysates were prepared, and in vitro kinase assays were performed essentially as described (Henkemeyer et al., 1994).

For biotinylation of cell-surface proteins, primary cultures of brain cells were obtained by treating postnatal day 4 (P_4) brains with trypsin/EDTA and plating in Dulbecco's modified Eagle's medium supplemented with 20% fetal calf serum. After 2 days, adherent cells were passaged onto two plates and allowed to recover for a further 2 days. The extracellular region of cell-surface proteins from these cultures was labeled with N-hydroxy succinimide–biotin (Calbiochem). Adherent cells were washed two times in phosphate-buffered saline (PBS) containing Ca^{2+} and Mg^{2+} and then incubated two times with rocking for 30 min each at room temperature in freshly diluted 0.5 mg/ml N-hydroxy succinimide–biotin in PBS containing Ca^{2+} and Mg^{2+}. Cells were washed by rocking for 10 min at room temperature in Dulbecco's modified Eagle's medium plus 10% fetal calf serum to quench excess N-hydroxy succinimide–biotin and then washed two times in PBS containing Ca^{2+} and Mg^{2+}. Cells were lysed in TxLB (1% Triton X-100, 138 mM NaCl, 20 mM Tris [pH 8.0], 2 mM EDTA, 10% glycerol, plus protease inhibitors) and protein concentrations determined by a bicinchoninic acid assay (Pierce). Immunoprecipitations were performed with 250 μg/ml of lysate and either anti-Nuk (Henkemeyer et al., 1994) or anti-βgal (Cappel #55976) rabbit antisera and Protein A-sepharose. Alternatively, avidin–agarose beads were used to precipitate biotinylated proteins. Immunoprecipitates were washed three times in TxLB, denatured, resolved on 8% polyacrylamide gels, and transferred to Immobilon-P membranes (Millipore). The membranes were blocked using 1% gelatin in TBST (0.05% Tween-20) and then Western-blotted in TBST plus 0.5% gelatin with avidin-HRP (BioRad, 1:50,000) followed by chemiluminescence (ECL, Amersham). Anti-βgal or anti-GAP (Ellis et al., 1990) Western blots utilized Protein-A-HRP (BioRad) as the secondary reagent.

Nuk-βgal Staining

For whole-mount staining, embryos were collected in 0.1 M PBS (pH 7.3), incubated at room temperature for 30 min in fresh lacZ fix buffer (0.2% gluteraldehyde, 5 mM EGTA, 2 mM $MgCl_2$ in PBS), rinsed several times in wash buffer (2 mM $MgCl_2$, 0.02% NP-40 in PBS), and incubated at 37°C overnight in lacZ staining buffer (wash buffer containing 1 mg/ml X-gal, 2.12 mg/ml potassium ferrocyanide, and 1.64 mg/ml potassium ferricyanide). Embryos were then rinsed in wash buffer, postfixed in formalin, dehydrated in an ethanol series, and cleared in benzyl alcohol:benzyl benzoate (1:2) immediately prior to observation and photography. For histochemical analysis, embryos were dehydrated in ethanol, embedded in paraffin, sectioned at 6 μm, and counterstained with nuclear-fast red.

For later stages of development, unfixed specimens were embedded in OCT and immediately cryosectioned at 15 μm. Air-dried sections were immersed in lacZ fix buffer for 8–10 min at room temperature, rinsed through multiple changes in wash buffer for 20 min, incubated at 37°C overnight in lacZ staining buffer, rinsed in wash buffer, postfixed in formalin, and counterstained with nuclear-fast red.

Bright-field photography was carried out with a Wild M10 macroscope or a Leitz DMRXE compound microscope using Kodak EPY 64 tungsten slide film.

Immunohistochemistry

Newborn mouse heads were fixed at 4°C for 24 hr in 4% paraformaldehyde in PBS, washed at 4°C in PBS, embedded in OCT, cryosectioned at 15 μm, and allowed to air dry overnight. Immunohistochemistry using 4 μg/ml of affinity-purified anti-Nuk antibodies (Henkemeyer et al., 1994) or anti-Lerk2 (A-20) antibodies (Santa Cruz Biochemicals) was performed with the ABC Elite detection system (Vector Laboratories).

Morphological Analysis of Mutant Brains

Adult mice were anesthetized and perfused with 20 ml PBS, followed by 40 ml of 4% paraformaldehyde. Tissues were then dissected, postfixed in 4% paraformaldehyde, equilibrated in 30% sucrose, and embedded in OCT, and 30 μm serial horizontal sections were obtained through the desired region using a Reichert-Jung model 2800 frigocut E cryostat. Samples were photographed using a Leitz wetzlar scope equipped with interference contrast optics mounted on a 360° rotating slide platform.

Dye Tracing of Mutant Brains

Axons forming the optic nerve were labeled by injecting approximately 1 μl of 1% rhodamine B dextran (Molecular Probes) into the retina of anesthesized adult mice through a microneedle that obliquely penetrated the corneal–scleral boundary. Axons forming the acA tract were labeled by injecting into anesthetized mice approximately 1 μl of 1% rhodamine B dextran into the anterior portion of the olfactory bulb. Axons forming the acP tract in adult mice were labeled by injecting into anesthetized mice 0.4–1.8 μl of 3% Fast Blue (Gross Umstat) stereotactically into the temporal cortex (0.5 mm ventral to the ventral boundary of the junction of the frontal and parietal bones, immediately anterior to the zygomatic arch; at an angle of 110° from the vertical, at a depth of 1.0 mm). Injected dye was allowed to trace axons in vivo in resuscitated animals for 48 hr. The animals were then perfused with paraformaldehyde, and serial sections through the appropriate brain tissue were obtained and viewed under fluorescence microscopy.

Acknowledgments

Correspondence should be addressed to T. P. We thank D. Rossi for assistance with ES cell cultures, K. Harpel for paraffin sections, T. Calzonetti for the pATG*lacZ* plasmid, and G. Yancopoulos and T. Hunter for discussion. Postdoctoral support for M. H. came from the Medical Research Council of Canada (MRC) and for J. T. H. from the Rick Hansen Society. Predoctoral support for T. M. S. came from an MRC studentship and for D. O. from an EMBL fellowship. This work was supported by a grant from Bristol-Myers-Squibb, a Terry Fox programme grant from the National Cancer Institute of Canada (NCIC), a Howard Hughes International Research Scholar Award to T. P., and a grant from the Deutsche Forschungsgemeinschaft to R. K. T. P. is a Terry Fox Cancer Research Scientist of the NCIC.

Received February 1, 1996; revised May 17, 1996.

References

Bartley, T.D., Hunt, R.W., Welcher, A.A., Boyle, W.J., Parker, V.P., Lindberg, R.A., Lu, H.S., Colombero, A.M., Elliott, R.L., Guthrie, B.A., and 10 others. (1994). B61 is a ligand for the ECK receptor protein–tyrosine kinase. Nature *368*, 558–560.

Beckmann, M.P., Cerretti, D.P., Baum, P., Vanden Bos, T., James, L., Farrah, T., Kozlosky, C., Hollingsworth, T., Shilling, H., Maraskovsky, E., Fletcher, F.A., Lhotak, V., Pawson, T., and Lyman, S.D. (1994). Molecular characterization of a family of ligands for the eph-related tyrosine kinase receptors. EMBO J. *13*, 3757–3762.

Bennett, B.D., Zeigler, F.C., Gu, Q., Fendly, B., Goddard, A.D., Gillett, N., and Matthews, W. (1995). Molecular cloning of a ligand for the EPH–related receptor protein–tyrosine kinase Htk. Proc. Natl. Acad. Sci. USA *92*, 1866–1870.

Bergemann, A.D., Cheng, H.J., Brambilla, R., Klein, R., and Flanagan, J.G. (1995). ELF-2, a new member of the Eph ligand family, is segmentally expressed in mouse embryos in the region of the hindbrain and newly forming somites. Mol. Cell. Biol. *15*, 4921–4929.

Brambilla, R., and Klein, R. (1995). Telling axons where to grow: a role for Eph receptor tyrosine kinases in guidance. Mol. Cell. Neurosci. *6*, 487–495.

Brambilla, R., Schnapp, A., Casagranda, F., Labrador, J.P., Bergemann, A.D., Flanagan, J.G., Pasquale, E.B., and Klein, R. (1995). Membrane-bound LERK2 ligand can signal through three different Eph-related receptor tyrosine kinases. EMBO J. *14*, 3116–3126.

Calzonetti, T., Stevenson, L., and Rossant, J. (1995). A novel regulatory region is required for trophoblast-specific transcription in transgenic mice. Dev. Biol. *171*, 615–626.

Cheng, H.J., and Flanagan, J.G. (1994). Identification and cloning of ELF-1, a developmentally expressed ligand for the Mek4 and Sek receptor tyrosine kinases. Cell *79*, 157–168.

Cheng, H.J., Nakamoto, M., Bergemann, A.D., and Flanagan, J.G. (1995). Complementary gradients in expression and binding of Elf-1 and Mek4 in development of the topographic retinotectal projection map. Cell *82*, 371–381.

Davis, S., Gale, N., Aldrich, T.H., Maisonpierre, P.C., Lhotak, V., Pawson, T., Goldfarb, M., and Yancopoulos, G.D. (1994). Ligands for the EPH–related receptor tyrosine kinases that require membrane attachment or clustering for activity. Science *266*, 816–819.

Dickson, B., and Hafen, E. (1994). Genetics of signal transduction in invertebrates. Curr. Opin. Genet. Dev. *4*, 64–70.

Drescher, U., Kremoser, C., Handwerker, C.J.L., Noda, M., and Bonhoeffer, F. (1995). In vitro guidance of retinal ganglion cell exons by RAGS, a 25 kDa tectal protein related to ligands for Eph receptor tyrosine kinases. Cell *82*, 359–370.

Ellis, C., Moran, M.F., McCormick, F., and Pawson, T. (1990). Phosphorylation of GAP and GAP–associated proteins by transforming and mitogenic tyrosine kinases. Nature *343*, 377–381.

Fletcher, F.A., Carpenter, M.K., Shilling, H., Baum, P., Ziegler, S.F., Gimpel, S., Hollingsworth, T., Vanden Bos, T., James, L., Hjerrild, K., Davison, B.L., Lyman, S.D., and Beckmann, M.P. (1994). Lerk-2, a binding protein for the receptor tyrosine kinase ELK, is evolutionarily conserved and expressed in a developmentally regulated pattern. Oncogene *9*, 3241–3247.

Henkemeyer, M., West, S.R., Gertler, F.B., and Hoffmann, F.M. (1990). A novel tyrosine kinase–independent function of Drosophila abl correlates with proper subcellular localization. Cell *63*, 949–960.

Henkemeyer, M., Marengere, L.E.M., McGlade, J., Olivier, J.P., Conlon, R.A., Holmyard, D.P., Letwin, K., and Pawson, T. (1994). Immunolocalization of the Nuk receptor tyrosine kinase suggests roles in segmental patterning of the brain and axonogenesis. Oncogene *9*, 1001–1014.

His, W. (1889). Die Formentwicklung des menschlichen Vorderhirns vom Ende des ersten bis zum Beginne des dritten Monates. Abhandl. D. Math. Phy. Kl. Kon Sachs. Akad. Wissench. Bd. *15*, 675–735.

Johnston, J.B. (1913). The morphology of the septum, hippocampus, and pallial commissures in reptiles and mammals. J. Comp. Neurol. *23*, 371–478.

Katz, M.J., Lasek, R.J., and Silver, J. (1983). Ontophyletics of the nervous system: development of the corpus callosum and evolution of axon tracts. Proc. Natl. Acad. Sci. USA *80*, 5936–5940.

Kozlosky, C.J., Maraskovsky, E., McCrew, J.T., Vanden Bos, T., Teppe, M., Lyman, S.D., Srinivasan, S., Fletcher, F.A., Gayle, R.B., III, Cerretti, D.P., and Beckmann, M.P. (1995). Ligands for the receptor tyrosine kinases hek and elk: isolation of cDNAs encoding a family of proteins. Oncogene *10*, 299–306.

Langelaan, J.W. (1908). On the development of the large commissures of the telencephalon in the human brain. Brain *31*, 221–241.

Letwin, K., Yee, S.-P., and Pawson, T. (1988). Novel protein–tyrosine kinase cDNAs related to *fps/fes* and *eph* cloned using antiphosphotyrosine antibody. Oncogene *3*, 621–627.

Lhotak, V., and Pawson, T. (1993). Biological and biochemical activities of a chimeric epidermal growth factor–ELK receptor tyrosine kinase. Mol. Cell. Biol. *13*, 7071–7079.

Lhotak, V., Greer, P., Letwin, K., and Pawson, T. (1991). Characterization of Elk, a brain-specific receptor tyrosine kinase. Mol. Cell. Biol. *11*, 2496–2502.

Mihalkovics, V. (1877). Entwicklungsgeschichte des Gehirns: Nach Untesuchungen an hoheren Wurbeltieren und den Menschen. (Leipzig: W. Engelmann.)

Nagy, A., Rossant, J., Nagy, R., Abramow-Newerly, W.A., and Roder, J.C. (1993). Derivation of completely cell culture–derived mice from early-passage embryonic stem cells. Proc. Natl. Acad. Sci. USA *90*, 8424–8428.

Pandey, A., Shao, H., Marks, R.M., Polverini, P.J., and Dixit, V.M. (1995). Role of B61, the ligand for the Eck receptor tyrosine kinase, in TNG-α–induced angiogenesis. Science *268*, 567–569.

Pawson, T., and Bernstein, A. (1990). Receptor tyrosine kinases: genetic evidence for their role in *Drosophila* and mouse development. Trends Genet. *6*, 350–356.

Probst, M. (1901). Uber den Bau des balkenlosen Grosshirns, sowie uber Mikrogyrie und Heterotopie der grauen Substanz. Arch. F. Psychiatr. *34*, 709–786.

Shao, H., Lou, L., Pandey, A., Pasquale, E.B., and Dixit, V.M. (1994). Cloning and characterization of a ligand for the Cek5 receptor protein–tyrosine kinase. J. Biol. Chem *269*, 26606–26609.

Shao, H., Lou, L., Pandey, A., Verderame, M.F., Siever, D.A., and Dixit, V. (1995). cDNA cloning and characterization of a Cek7 receptor protein–tyrosine kinase ligand that is identical to the ligand (ELF-1) for the Mek4 and Sek receptor protein–tyrosine kinases. J. Biol. Chem. *270*, 3467–3470.

Silver, J., Lorenz, S.E., Wahlsten, D., and Coughlin, J. (1982). Axonal guidance during development of the great cerebral commissures: descriptive and experimental studies, in vivo, on the role of preformed glial pathways. J. Comp. Neurol. *210*, 10–29.

Suitsu, N. (1920). Comparative studies on the growth of the corpus callosum. J. Comp. Neurol. *32*, 35–60.

Tessier-Lavigne, M. (1995). Eph receptor tyrosine kinases, axon repulsion, and the development of topographic maps. Cell *82*, 345–348.

Tuzi, N.L., and Gullick, W.J. (1994). Eph, the largest known family of putative growth factor receptors. Br. J. Cancer *69*, 417–421.

Tybulewicz, V.L.J., Crawford, C.E., Jackson, P.K., Bronson, R.T., and Mulligan, R.C. (1991). Neonatal lethality and lymphopenia in mice with a homozygous disruption of the c-abl proto-oncogene. Cell *65*, 1153–1163.

Von Szily, A. (1912). Uber die einleitenden Vorgange bei der ersten Entstehung der nervenfasern im nervous opticus. Graefes Arch. Opthalmol. *81*, 67–86.

Winslow, J.W., Moran, P., Valverde, J.A.S., Yuan, J.Q., Wong, S.C., Tsai, S.P., Goddard, A., Henzel, W.J., Hefti, F., Beck, K.D., and Caras, I.W. (1995). Cloning of AL-1, a ligand for an Eph-related tyrosine kinase receptor involved in axon bundle formation. Neuron *14*, 973–981.

Wurst, W., and Joyner, A.L. (1993). Gene Targeting: A Practical Approach. (Cambridge: Oxford University Press).

Xu, Q., Alldus, G., Holder, N., and Wilkinson, D.G. (1995). Expression of truncated Sek-1 receptor tyrosine kinase disrupts the segmental restriction of gene expression in the *Xenopus* and zebrafish hindbrain. Development *121*, 4005–4016.

Note Added in Proof

The data referred to throughout as Gale et al., submitted, are now in press: Gale, N.W., Holland, S.J., Valenzuela, D.M., Flenniken, A., Pan, L., Ryan, T.E., Henkemeyer, M., Strebhardt, K., Hirai, H., Wilkinson, D.G., Pawson, T., Davis, S., and Yancopoulos, G.D. Eph receptors and ligands comprise two major specificity subclasses and are reciprocally compartmentalized during embryogenesis. Neuron *17*, in press.